Earth-fault detection and localization in isolated industrial MV network – comparison of directional overcurrent protection and signal injection method

Nina Stipetic, Bozidar Filipovic-Grcic, Ivo Uglesic, Alain Xémard, Naum Andres

***Abstract* - Neutral earthing directly affects systems' behaviour regarding the maximum level of earth-fault current and overvoltages. Isolated neutral is used where continuity of power supply is essential, which is often the case in industrial power utilities. Although the system can remain in service during a single-phase earth-fault, locating the fault should be done as quickly as possible, without disrupting the operation of the loads. Directional earth-fault protection (67N) can be used to indicate the faulty feeder. An alternative method is low-frequency (LF) current injection combined with sensors for detecting the injected signal, which is a known technique used in LV systems. In this paper, the application of 67N protection and the LF current injection method are tested on the same MV system with inaccessible neutral point. Inductive voltage transformers (IVTs) are used for signal injection. Both methods are discussed, and their limitations are compared based on simulation results obtained using the model of an isolated MV industrial plant. The model includes relay protection devices and IVTs for signal injection.**

***Keywords*: isolated network, earth-fault, directional earth-fault protection, low-frequency signal injection.**

I. Introduction

Continuity of service is the main advantage of systems with isolated neutral, such as small industrial networks. The earth-fault current in such network finds its path through systems' capacitances to ground and does not lead to a high fault current. Nevertheless, it is important to locate the fault as soon as possible to restrain the overvoltage stress of the healthy phases and to prevent the occurrence of a second fault that would require switching [1][2]. In practice, in isolated industrial MV networks, the conventional solution is to use permanent insulation monitors (PIMs) connected between systems' artificial neutral and earth. Based on DC injection, PIMs calculate the total systems' insulation resistance and indicate its decrease when an earth-fault occurs. Since the location of the fault remains unknown, detecting the faulty line is done by sequentially opening of the feeder breakers, which is time consuming and inconvenient for industrial networks where continuity of supply is of great importance. Sequential opening of the feeder breakers produces switching overvoltages which might have negative effects on insulation systems of equipment or even in some cases lead to fault caused by resonant overvoltages.

A lot of research is done on the subject of fault localization mainly in distribution systems [3-4], especially in unearthed or compensated networks where the fault localization is more challenging. The numerous proposed techniques are usually classified as fundamental frequency phasor measurement methods [5-10], transients and high frequency measurement methods [11-16], signal injection and tracking methods [15-24] and recently proposed special methods such as fault localization based on artificial intelligence [26-28] or fault localization combined with partial discharge sensors [29-30].

In practice, for small industrial networks, earth-fault directional overcurrent protection 67N based on fundamental frequency phasor measurements is widely used to identify the faulty line. 67N protection requires usage of numerical relays and appropriate current transformers on each feeder, whose sensitivity thresholds are the limitation for this method. Considering the required equipment, the directional overcurrent protection is a reasonable solution for power plants that are to be newly built or reconstructed.

The signal injection method is used in LV isolated system, where the direct signal injection between the systems' neutral and earth is possible. At MV level, this method has received limited attention. However, it was proposed and tested in compensated networks [19-22] where the signal injection was done using the Petersen coil. In [19], injection using the arc suppression coil auxiliary winding is described. The developed prototype of the tracking sensor was successfully tested, but no injection circuit, limits in terms of fault resistance, grounding impedance, or arc suppression coil winding have been discussed. In [20-21] a rectangle pulse and fast pulse injection method in compensated network are described and field tested on a 20 kV test network. The rectangle pulsing current can be easily generated by switching capacity on and off in parallel to the Petersen coil and the faulty feeder is determined by the rms value of the zero-sequence current. Due to several drawbacks (the network must be overcompensated, the fault must be constant for 25 s to detect pulses, works only in small networks because the overcompensation cannot be increased to any network size…), the fast pulse method was proposed. The thyristor controlled pulse generator was introduced to generate defined short pulses, which reduced the time to detect the faulty segment. The method can detect faults with fault-impedances up to 400 Ω and combined with information about the zero-

N. Stipetic, B. Filipovic-Grcic and I. Uglesic are with University of Zagreb, Faculty of Electrical Engineering and Computing, 10000 Zagreb, Croatia (e-mail of corresponding author: nina.stipetic@fer.hr)
A. Xémard is with Électricité de France, 91120 Palaiseau, France
N. Andres is with Électricité de France, 69007 Lyon, France

Paper submitted to the International Conference on Power Systems Transients (IPST2021) in Belo Horizonte, Brazil June 6-10, 2021.

sequence voltage it works up to 10 kΩ [23]. In [24], signal injection using a VT is proposed. However, an indirectly earthed distribution system is again discussed, injection is done to the faulty phase only, fault resistances up to 300 Ω were simulated and the emphasis is given to impedance-based calculation of the fault distance. In [25] a zero-sequence current carrier signal injection via current transformer (CT) was proposed and the method is applicable for both compensated and isolated networks. The zero-sequence currents are modulated with different frequencies on the secondaries of CTs using high frequency electronic switches which enable or disable the burden resistance to be connected or short circuited. The modulated zero sequence carrier signal is injected to the feeders and propagate to the substation for filter treatment and specific frequency detection. The simulations and experimental laboratory model tests verified the correctness of the proposed method; however, no fault resistance was mentioned and different high frequencies for modulation at different CTs seem rather complex for implementation.

There was a little research focused on signal injection method in MV isolated networks and in [3] and [9] it is even stated that injection method is limited to compensated networks. In this paper, a new proposition for signal injection method application in industrial isolated network is presented. Based on working principle of a PIM, the injection circuit using the existing IVTs is proposed for LF sinusoidal signal injection.

The paper firstly gives a brief overview of the 67N protection and LF injection method. Then the EMTP model of an isolated MV industrial network used in power plants that was used in simulations is described. Finally, the possibility of fault detection in terms of the resistance at the fault location is simulated. The simulation results for the 67N protection and LF injection method are presented and discussed.

A. Earth-fault directional overcurrent protection

During an earth-fault, the zero-sequence voltage rises and zero-sequence current flows in the system. The zero-sequence voltage is the same regardless of location, while the zero-sequence current will have a different magnitude throughout the network. Since the zero-sequence current in isolated network is relatively small, it may be problematic to achieve selective protection. To distinguish the fault current from the capacitive current of a healthy feeder, directional overcurrent protection uses both zero-sequence voltage and current to detect earth faults. It is based on two functionalities: overcurrent and direction, i.e., if the fault current is above the setting threshold and if its phase displacement in relation to a zero-sequence voltage is inside a pre-defined zone, the protective device on the faulty feeder will indicate the earth fault [1], [31]. The general recommendation is to set the threshold of overcurrent protections higher than 12 % of the rated current of the current transformer (CT) if measurements are done by 3 CTs, or above 1 A if measurements done by core-balance current transformers (CBCTs) [1]. Aside from this recommendation, calculation can be made to relate the earth-fault magnitudes to the exact relay overcurrent threshold and ensure that relay will be able to successfully detect any earth-fault in a particular network.

B. Low-frequency signal injection technique

Signal injection for fault location can be done in different ways, depending on the characteristics of the injected signal (sinusoidal, DC, pulse), device used for injecting the signal (depends on the grounding option) and devices used for detecting the signal (mobile detectors, instrument transformers, Hall sensors). In isolated MV networks fed by a transformer with a delta winding, the neutral is not accessible. In this case, the injection device can be connected between phases and earth using voltage transformers. As shown in Fig. 1, a LF signal generator injects current through the primary windings of IVTs which are grounded over a capacitor to avoid current being shunted. The secondaries of three-winding voltage transformers are used for measurement and are loaded with rated load. The tertiary is delta-connected and loaded with resistor to damp the ferroresonance phenomena [32].

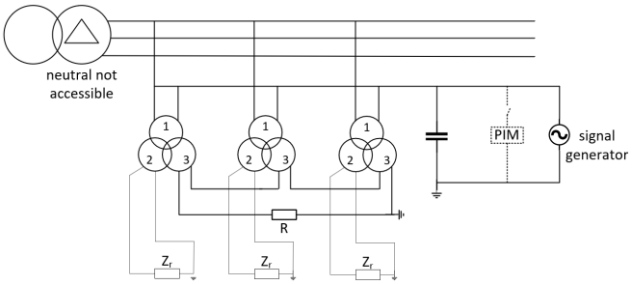

Fig. 1. Schematic preview of signal injection into isolated MV network using the primary windings of IVTs

Several considerations are important for sinusoidal injection. LF is used to reduce the influence of network capacitances on the injected current distribution. Since the capacitive reactance of the network is high at low frequencies, the lower the frequency of the injected current, the higher the possibility it will close its path through the resistance at fault location. On the other hand, the higher the injection signal magnitude, the easier the detection by current sensors. Regarding the IVTs, the induced voltage in the IVT is described by the following equation:

$$E_{rms} = 4.44 \cdot N \cdot f \cdot \Phi_{max} \rightarrow \quad \Phi_{max} = \frac{E_{rms}}{4.44 \cdot f \cdot N} \qquad (1)$$

where, ϕ is the core magnetic flux, E is the induced voltage and N is the number of turns. Observing the equation (1) it is clear that a change in the ratio E/f results in a change in the flux ϕ. If the applied voltage remains the same, the induced voltage will remain the same and decrease of the frequency will result in an increase of the flux. If the frequency is held constant, an increase in the magnitude of the injected signal will result in an increase of the flux. Increasing the flux over the knee point of the current-flux curve will lead to core saturation which increases the current through the primary winding and this should generally be avoided. Therefore, the injection signal parameters should be carefully chosen to avoid excessive flux increase. If the IVT occasionally enters saturation, care should be taken to ensure that the primary current does not thermally overload the primary windings. The advantage of this method is that the parameters of the injected signal are controllable and can be adjusted on-site. Another advantage is that the injection

is not permanent, but lasts from the fault indication to fault location, and it is assumed that any short-term saturations will not affect the IVT condition.

II. MV Network Model Used for Simulations

Earth-fault and fault detection simulation is performed in EMTPWorks 4.0 on an example of an industrial 10.5 kV network commonly used in power plants. The network consists of 6 buses (A-F) with several feeders connected. The feeders are modelled using the pi-model equivalent and their lengths vary from 14 m to 300 m. Eight asynchronous machines with ratings ranging from 0.6 MVA to 13 MVA are connected to the MV network, and the centrifugal type loads are described by torque-speed characteristics. The motor capacitances are not neglected as they are important for the earth-fault simulation. The relevant parameters of the feeders and loads are given in the Appendix I. The total earth-fault current is independent of the fault location. For the described network it equals 21.4 A_{rms} in the case without earth-fault resistance. However, possible reduced network topologies should be considered for setting the earth-fault protection. During the low-power scenario, not all loads and feeders are connected, but an earth-fault may still occur, resulting in even lower fault-current magnitude due to the reduced network capacitance. Considering the low-power scenario of the studied network, the topology shown in Fig. 2 was used for further earth-fault simulations. The total earth-fault current for low-power scenario, in the case without fault resistance, is 6.5 A_{rms}.

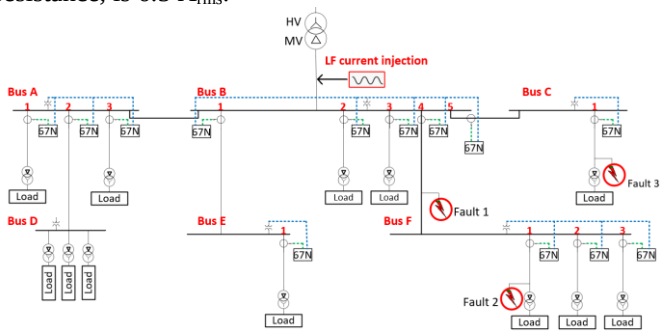

Fig. 2. Reduced network topology for low-power scenario used in earth-fault simulations

III. Simulation Results – Directional Overcurrent Earth-Fault Protection

For the simulation of directional earth-fault protection, the secondary circuit is modelled using the available relay model 50-51-67 from the EMTP Protection Toolbox library. The relay input on each feeder is the corresponding residual current. Conducted simulations considered different fault locations. The residual currents at MV level at each feeder are given in Table I. For each feeder there are two residual current values, for the case when it is healthy or the faulty one.

The residual current of a healthy feeder is proportional to its capacitance. Residual current of the faulty feeder is proportional to the difference of the total system capacitance and the capacitance of the faulty feeder, according to equation:

$$I_{rsdf} = 3j(C - C_f)\omega V_n \quad (2)$$

where, C is the total system capacitance per phase, C_f is the faulty feeder capacitance per phase and V_n is the neutral point potential.

TABLE I
Residual Currents on Feeders in Healthy Condition and in Case of a Solid Earth-Fault

BUS	*Feeder*	*Length*	I_{res_prim} *HEALTHY*	I_{res_prim} *FAULTY*
A	A1	260 m	0.424 A	6.090 A
	A2 (A to D)	179 m	0.654 A	5.860 A
	A3	38 m	0.062 A	6.090 A
B	B1 (B to E)	2 x 260 m	2.006 A	4.513 A
	B2	36 m	0.059 A	6.461 A
	B3	22 m	0.036 A	6.484 A
	B4 (B to F)	2 x 260 m	2.160 A	4.360 A
	B5 (B to C)	300 m	1.120 A	5.400 A
C	C1	14 m	0.023 A	6.497 A
E	E1	2 x 32 m	0.104 A	6.414 A
F	F1	2 x 23 m	0.075A	6.444 A
	F2	2 x 29 m	0.095A	6.424 A
	F3	2 x 27 m	0.088 A	6.431 A

Therefore, the lowest residual current on a faulty feeder is expected to be on the feeder with the largest capacitance, i.e. the feeder with greatest residual current in healthy condition. As observed from Table I, compared to other healthy feeders, all connecting feeders have greater residual currents in healthy condition since they are longer, they have greater capacitance per length, and they connect a larger subnetwork. Cable data is given in Table IV in the Appendix. Out of all connecting feeders, B4 has the highest residual current in healthy state, and lowest residual current in faulty state. Therefore, the fault at feeder B4 in low power scenario is relevant for the sensitivity setting of the directional overcurrent protection.

A. Current transformer considerations

There are two important considerations in managing the protection settings: the relay input threshold and the current transformer accuracy. It can generally be assumed that the threshold for the relay current input signal is 30 mA, or 1 mA if the sensitive input and CBCT is used [33]. Depending on the primary current magnitude, CTs can cause errors in ratio and phase displacement, bringing the magnitude and the phase of the secondary current to question. The IEC standard [34] defines the accuracy classes 0.1, 0.2, 0.2S, 0.5, 0.5S, 1, 3, 5 for measuring CTs and several protective classes. Classes 0.1, 0.2, 0.5 and 1 specify the accuracy down to 5% of rated current. The 0.2S and 0.5S accuracy classes extend down to 1 % of rated current. For magnitudes lower than 1 % (5 %) of the rated current there is no standardized error or any guarantee on the CT ratio accuracy.

Magnitudes and the values of residual currents on the CT secondary depending on the CT ratio are shown in Table II. In the full topology case, the magnitudes on the secondary side are high enough for the relay without using the sensitive input. However, the accuracy of the CT is questionable, since the residual current at primary side is too low. For the low-power scenario it is obvious that sensitive relay input must be used, which implies the usage of CBCTs as measuring devices. The rated primary current of the CBCT must be higher than the

maximal residual current and at the same time as low as possible to improve the sensitivity.

TABLE II
COMPARISON OF THE LOWEST RESIDUAL CURRENT MAGNITUDES ON THE FAULTY FEEDER AT PRIMARY AND SECONDARY SIDE OF THE CT/CBCT, DEPENDING ON THE T RATIO

	PRIMARY	***SECONDARY***			
	Min. I_{resF}	*CT ratio 2500:1*	*CT ratio 2500:5*	*CBCT 70:1*	*CBCT 100:1*
Full topology, 100 % P	16.33 A	6.5 mA	32.7 mA	233.3 mA	163.3 mA
Low power scenario	4.36 A	1.7 mA	8.7 mA	62.3 mA	43.6 mA

B. Influence of fault resistance

The fault resistance lowers the earth-fault current magnitude which affects the sensitivity setting of the protective device. The maximum fault resistance for which the fault is still detectable is the one that reduces the fault current to the level of relay sensitivity threshold. To find the maximum earth fault resistance for which the relays will remain sensitive, the case where the fault causes the lowest residual current magnitude is again relevant.

To find the theoretical limitation in terms of detectable high resistance fault, all relays were set to be as sensitive as possible. First, the relays' thresholds were set to 30 mA, and the simulations of the earth fault at the end of connecting feeder B4 were repeated, while increasing the earth fault resistance. Once the maximum value for the sensitivity of 30 mA was found, the process was repeated for the sensitive relay input with a setting of I_{pkp} of 1 mA. The relation between the residual current on the faulty feeder at CBCT's secondary and the earth fault resistance for the lowest possible threshold (considering ideal CBCT) are given in Fig. 3 and Fig. 4.

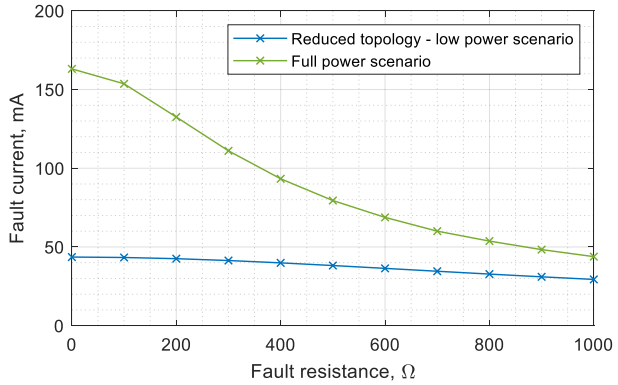

Fig. 3. Residual current on the faulty feeder B4 – the secondary current of the CBCT in relation to the fault resistance varied from 0 Ω to 1 kΩ

According to the simulation results, the maximum earth fault resistances for relay thresholds of 30 mA and 1 mA are 960 Ω and 39865 Ω, respectively. However, it is not advisable to set the relays to maximal sensitivity since there is a risk of spurious tripping (for example motor starting, transients due to other faults, etc.). If the earth fault occurs at any other feeder, for the same relay pick-up setting, the fault resistances can be even higher since previous simulations showed higher residual currents for faults on other feeders.

To consider the CBCT accuracy, the sensitivity thresholds should be increased for the amount of transformation error. If the rated primary current of the CBCT is 100 A, the error in the measuring range of 30 mA and 1 mA at secondary is 0.75 % and 1.5 % for classes 0.2S and 0.5S respectively.

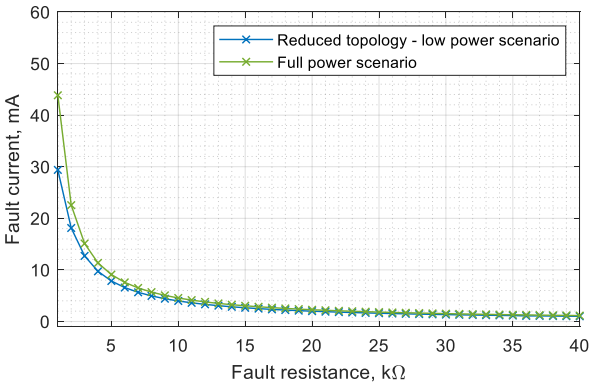

Fig. 4. Residual current on the faulty feeder B4 – the secondary current of the CBCT in relation to the fault resistance varied from 1 kΩ to 40 kΩ

These errors at very low current range will not affect the maximum fault resistance significantly. To be on the safe side, one can consider the CBCT measuring error of 10 %. For the transformation error of 10 %, the thresholds considered are 33 mA and 1.1 mA, which lowers the detectable fault resistances in the reduced topology to 850 Ω and 35 kΩ.
The use of a measurement CBCT with a relay having a sensitive input considerably increases the impedance of detected faults.

IV. SIMULATION RESULTS – LOW-FREQUENCY SIGNAL INJECTION

To simulate the low-frequency current injection, the same network configuration was considered. According to the scheme in Fig. 1, the circuit for injection was modelled in EMTP (Fig. 5) and connected to the network model as indicated in Fig. 2. The IVT data used is available in Table VI in the Appendix.

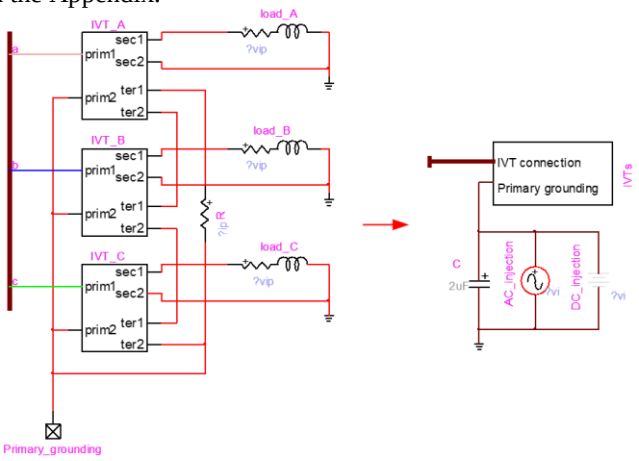

Fig. 5. Three-phase three-winding IVTs connection and the circuit for current injection modelled in EMTP

Firstly, a DC injection was tested for total insulation resistance calculation. A clear drop from 705 kΩ to 0.584 kΩ was observed after the occurrence of a solid earth-fault. This confirmed the good functioning of a PIM, which triggers an alarm when a total insulation resistance drops under a predefined value in order to continue with AC signal injection for fault localization. The frequency of 2.5 Hz was chosen for

injection, following the practice for fault tracking in LV systems [1], [35]. The harmonic analysis of the residual current on all feeders is done to determine the faulty feeder. Earth-fault was simulated at Fault 1, Fault 2 and Fault 3 locations indicated in Fig. 2: at a connecting feeder B4, deeper in the network at the ending feeder F1 and on the shortest feeder in the network, C1, which is 14 m long. Simulations showed that the 2.5 Hz component of residual current is traceable for each fault location and is always the highest on a faulty feeder compared to all other healthy feeders.

Fig. 6 shows the comparison of the primary IVT current for 2.5 Hz, 100 V, 200 V and 300 V injection in case of a solid earth-fault. From the primary current waveform, it can be observed that the IVT gets saturated for 200 V and 300 V injections.

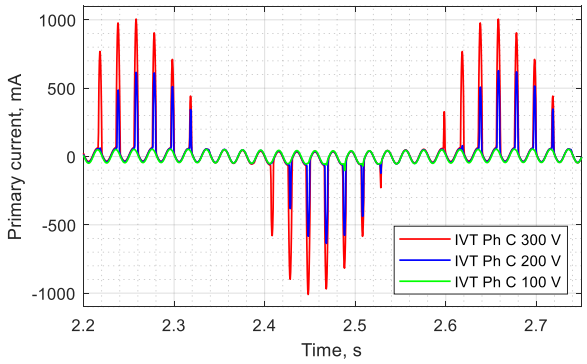

Fig. 6. Comparison of primary currents of IVT during the earth-fault in case of AC voltage source magnitudes of 100 V, 200 V and 300 V

For 100 V injection, there is no saturation and the magnitude of 2.5 Hz component in the residual current on the faulty feeder is 19.5 mA, which is high enough for detection by leakage current clamps. Increasing the injection magnitude increases the magnitude of the 2.5 Hz component in the residual current on the faulty feeder and prolongs the saturation time. However, for 300 V injection, the saturation is still periodical and should not be detrimental to IVTs, especially because the AC injection is not constant, but only lasts for the short time period needed to locate the fault. Table III shows the 2.5 Hz residual current magnitudes at faulty feeder, currents and maximum magnetic flux related to the IVT for the aforementioned injections. The secondary and tertiary currents increase only slightly and do not represent limitations as long as the thermal limit for the windings is not reached.

TABLE III
COMPARISON OF RELEVANT PARAMETERS IN STEADY-STATE DURING SOLID EARTH-FAULT

2.5 Hz inj. signal magnitude [V]	2.5 Hz magnitude of $3I_0$ at faulty feeder [mA]	I_{prim} [mA]	Φ_{max} [Wb]	saturation
100	19.5	75	55.2	no
200	127.8	625	62.3	periodically
300	280.3	1005	67.38	periodically, longer duration

A. Influence of fault resistance and injection frequency

The fault resistance was considered again to check the effect of increasing fault resistance on the 2.5 Hz magnitude of the residual current. The idea is to increase the fault resistance until the clamps' sensitivity of 1 mA is reached. However, the increasing fault resistance affects the fault current distribution. For the Fault 1 location, even for the very high fault resistance of 100 kΩ (approaching steady-state according to current and voltage values, but a total insulation resistance decrease is still observed after DC injection), the 2.5 Hz component magnitude of the residual current is still the highest on feeder B4 and it equals 4.71 mA. For faults on other feeders, the distribution of the fault current is such that, at some point, the faulty feeder has no longer the highest 2.5 Hz component magnitude. Fig. 7 shows the 2.5 Hz component magnitude of residual current at faulty feeder for the fault on the shortest feeder C1.

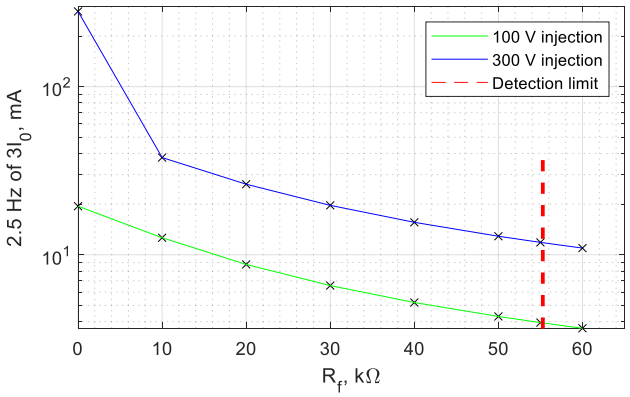

Fig. 7. 2.5 Hz component of $3I_0$ at faulty feeder C1 vs R_f

For fault resistance lower than 55 kΩ, the faulty feeder can be determined since the 2.5 Hz component is the highest on the feeder C1 and its connecting feeder B5. However, for higher fault resistances, the 2.5 Hz component magnitude is again the highest on feeder B4 (whose capacitance is the highest) and comparing the 2.5 Hz component magnitudes does not lead to the faulty feeder determination. Increasing the injection frequency to 10 Hz lowers residual current magnitude on faulty feeder, and the fault resistance for which the fault is still detectable, as shown in Fig 8.

Higher fault resistances lower the injection current and the primary winding IVT current so the IVT core does not get saturated as in the case of solid earth-fault. Reduction in topology also lowers the total injection current which is favourable for the IVT.

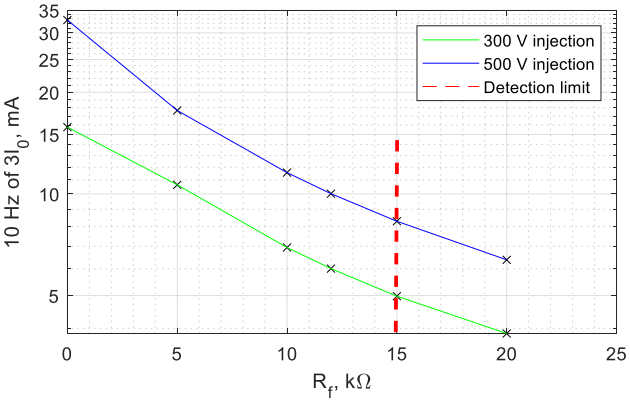

Fig. 8. 10 Hz component of $3I_0$ at faulty feeder C1 vs R_f

V. Discussion

The 67N protection is a commercially available solution that is used in practice. It is a reasonable solution for industrial or power plants that are to be newly built or reconstructed. The network in such plants is not large compared to distribution networks, and the total capacitance is smaller which leads to lower fault current magnitudes. The sensitive earth-fault protection and CBCT are most probably required in such networks. The exact sensitivity margin of a relay for a particular topology can be calculated. For the studied network, if the theoretically maximal sensitivity is considered, faults up to 35 kΩ can be detected on the feeder with lowest residual current. Application of 67N protection requires installation of numerical relays and CBCTs on each feeder.

LF signal injection was considered thinking of existing plants that are not equipped for directional overcurrent protection. At the moment, there is no on-the-shelf LF signal injection solution for isolated MV networks. In this paper, the LF current injection using the configuration of three three-winding IVTs was proposed. Simulations showed that the injected signal is traceable throughout the network and can be used for faulty feeder identification. The magnitudes of the injected signal at faulty feeders are shown to be high enough for current clamps whose frequency range should cover the injected frequency signal. The convenience of the method is that the injection signal parameters can be adjusted until appropriate for faulty feeder determination. This is especially important considering the resonant frequencies of the network, which can be determined by conducting a frequency scan in EMTP. If the frequency of injected current is close to the resonant frequency, another injection frequency can be chosen. The clamps can have the built-in logic to sense the particular frequency or could be connected to external power analyzer or oscilloscope for further analysis. Considering the required equipment, the injection method might be more convenient for older plants without special earth-fault detection solutions.

Simulations have shown that it is possible to detect faults with higher fault resistances compared to 67N protection for the observed network. For very high fault resistances that are at detectability margin due to the influence of the network capacitance and injected current distribution, comparison of the residual currents during the signal injection, but before and after the fault can be helpful. The feeder at which the difference in residual current magnitude occurs after the fault occurrence is the faulty one.

The proposed method was tested on the purely cable network model, but it is theoretically applicable to mixed-networks. Compared to cables, overhead lines have lower capacitance per length. This results in lower residual currents on healthy overhead lines during the fault which affects the sensitivity setting of conventional earth-fault protection. Possible phase-to-earth capacitance unbalance may also affect the false tripping of earth-fault protection. On the other hand, in favour of the injection method, smaller capacitances result in greater capacitive reactance which enlarges the portion of injected LF current that will close its path through the fault location. The proposed method has advantages regarding the possible unbalances in the network and changing the network topology and should work in both cable and overhead line networks. Simulation of the injection method into a larger, mixed cable-overhead line network is planned in further research in order to find the limit regarding the network size and dependency on cable and overhead line ratio in the network

The critical component in the injection circuit is the IVT, whose critical parameters were analysed. Depending on the injection current magnitude and frequency, the injection can bring IVT's core to saturation. Saturation is immediately detectable from the injected current waveform. For further research, dimensioning and development of the special IVT will be considered. Higher knee-point in the current-flux characteristic or higher current thermal capability of the primary windings will allow injection of the signal with higher magnitudes without saturating the IVT core.

VI. Conclusions

The paper deals with the earth-fault detection in the isolated MV network of an industrial plant. Two fault location techniques are discussed and simulated on the same network: directional overcurrent protection and low-frequency signal injection. The latter one is applied in LV systems using PIMs, but there is no solution for MV level. It is shown how the residual current magnitude affects the selection of residual current measuring device. Depending on the lowest residual current in the network in the low-power scenario a relay sensitivity threshold was found for a solid earth-fault and additionally expressed in terms of maximum fault resistance allowed to retain the relays' sensitivity. The lowest possible threshold setting is not advisable to avoid false tripping. A low-frequency signal injection technique through IVTs is tested in the paper. It showed signal traceability in the network and better results in terms of detecting high resistance faults. The injection method requires less equipment for the faulty feeder identification and is unaffected by the possible unbalances in the network.

VII. Appendix

TABLE IV
Feeder Data at 50 Hz

	R (Ω/km)	X (Ω/km)	C (μF/km)	G (S/km)
Connecting cable	0.06	0.09	0.65	$2.17 \cdot 10^{-11}$
Other feeders	0.41	0.11	0.29	$1.05 \cdot 10^{-11}$

TABLE V
Motor Data

Motor	S_n (MVA)	C (μF)	Motor	S_n (MVA)	C (μF)
B1	3	0.100	E2	1	0.800
B2	3.4	0.457	F1	0.6	0.085
C1	0.9	0.152	F2	0.9	0.085
E1	9	0.160	F3	0.9	0.152

TABLE VI
Inductive Voltage Transformer Data

IVT Data	U_{nRMS} (V)	S_n (VA)	I_{nRMS}	R	L''_σ (mH)	X''_σ (mH)
Primary	$10500/\sqrt{3}$		8.25 mA	1753.12 Ω	0.75	235.82
Secondary	$10500/\sqrt{3}$	50	0.87 A	126.6 mΩ		
Tertiary	100/3	25	0.75 A	166.26 mΩ	0.36	171.71

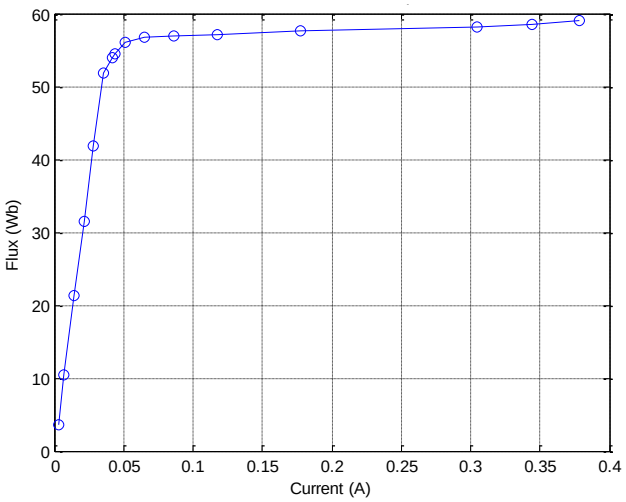

Fig. 9. Flux-current curve of the IVT used for modelling

VIII. REFERENCES

[1] C. Prévé, Protection of Electrical Networks, ISTE Ltd, 2006

[2] F. Jullien, I. Héritier, "The IT earthing system in LV", Schneider Electric Collection Technique, Cachier Technique no. 178, first issue, June 1999

[3] A. Farughian, L. Kumulainen, K. Kauhainiemi, "Review of methodologies for earth fault indication and location in compensated and unearthed MV distribution networks", EPSR 154 (2018) 373-380

[4] M. Shafiullah, M. Abido, "A review on distribution grid fault location techniques", Electric Power Components and Systems (2017) 0, 1-18

[5] A. H. A. Bakar, B. Ooi, P. Govindasamy, C. Tan, H. A. Illias, and H. Mokhlis, "Directional overcurrent and earth-fault protections for a biomass microgrid system in Malaysia", Int. J. Electr. Power Energy Syst., vol. 55, pp. 581–591, 2014.

[6] J. Altonen, A. Wahlroos, "Advancements in fundamental frequency impedance based earth-fault location in unearthed distribution systems", CIRED 19th International Conference on Electricity Distribution, Vienna , Austria 2007

[7] J. Horak, "Directional Overcurrent Relaying (67) Concepts", 59th Annual Conference for Protective Relay Engineers, 2006., College Station. TX, USA

[8] K. Lowczowski, J. Lorenc, J. Andruszkiewicz, Z. Nadolny, J. Zawodniak, "Novel Earth Fault Protection Algorithm Based on MV Cable Screen Zero Sequence Current Filter", Energies 2019, 12(16), 3190

[9] A. Farughian, L. Kumpulainen, K. Kauhaniemi, "Earth Fault Location Using Negative Sequence Currents", Energies 2019, 12(19), 3759

[10] A. Farughian, L. Kumpulainen, K. Kauhaniemi, "Non-Directional Earth Fault Passage Indication in Isolated Neutral Distribution Networks", Energies 2020, 13(18), 4732

[11] X. Lin, S. Ke, Y. Gao, B. Wang, and P. Liu, "A selective single-phase-to-ground fault protection for neutral un-effectively grounded systems," Int. J. Electr. Power Energy Syst., vol. 33, no. 4, pp. 1012–1017, 2011.

[12] M. M. Alamuti, H. Nouri, R. M. Ciric, and V. Terzija, "Intermittent fault location in distribution feeders", IEEE Trans. Power Deliv., vol. 27, no. 1, pp. 96–103, 2012.

[13] I. Xyngi, M. Popov, "Transient Directional Busbar Protection Scheme for Distribution Networks", 10th IET International Conference on Developments in Power System Protection (DPSP 2010), Manchester

[14] M. R. Adzman, "Earth Fault Distance Computation Methods Based on Transients in Power Distribution Systems", Doctoral Dissertation 189/2014, Aalto University, Finland

[15] N.I. Elkalashy, N.A. Sabiha, M. Lehtonen, "Earth Fault Distance Estimation Using Active Traveling Waves in Energized-Compensated MV Networks", IEEE Transactions on Power Delivery, Volume: 30, Issue: 2, 836 – 843, April 2015

[16] G. Druml, G. Achleitner, W. Leitner, L. Fickert, "New single-ended earthfault distance estimation for the 110 kV and 20 kV-compensated network", Elektrotechnik & Informationstechnik (2018) 135/8: 567–575

[17] Z. Wang, Y. Qi, "Study and Realizing of Method of AC Locating Fault in Distribution System, 2010 Asia-Pacific Power and Energy Engineering Conference, Chengdu, China

[18] G. Buigues, V. Valverde, I. Zamora, J. Mazón, and E. Torres, "Signal injection techniques for fault location in distribution networks", Renew. Energy Power Qual. J., vol. 1, no. 10, pp. 412–417, 2012.

[19] C. Raunig, L. Fickert, C. Obkircher, and G. Achleitner, "Mobile earth fault localization by tracing current injection", 7th Int. Conf. Electr. Power Qual. Supply Reliab. Conf. Proc., pp. 243–246, 2010., Kuressaare, Estonia

[20] G. Druml, C. Raunig, P. Schegner, L. Fickert, "Fast selective earth fault localization using the new fast pulse detection method", 22nd International Conference on Electricity Distribution, 2013, Stockolm, Sweden

[21] G. Druml, C. Raunig, L. Fickert, "Earth Fault Localization with the Help of the Fast-Pulse-Detection-Method using the New High-Power-Current-Injection (HPCI)", Electric Power Quality and Supply Reliability, 2012 Tartu, Estonia

[22] G. Druml, C. Raunig, P. Schegner, L. Fickert, "Fast selective earth fault localization using the new fast pulse detection method", 22nd International Conference on Electricity Distribution, 2013, Stockolm, Sweden

[23] C. Tengg, K. Schoass, G. Druml, R. Schmaranz, M. Marketz, L. Fickert, "Evaluation of new earth fault localization methods by earth fault experiments", 22nd International Conference on Electricity Distribution, 2013, Stockolm, Sweden

[24] Y. Bai, W. Cong, J. Li, L. Ding, Q. Lu, and N. Yang, "Single phase to earth fault location method in distribution network based on signal injection principle", DRPT 2011 - 2011 4th Int. Conf. Electr. Util. Deregul. Restruct. Power Technol., no. 50807032, pp. 204–208, 2011.

[25] B. Chen, N. Yu, B. Chen, C. Tian, Y. Chen, G. Ghen, "Fault Location for Underground Cables in Underground MV Distribution Networks Based on ZSC Signal Injection", IEEE Transactions on Power Delivery 2020, 1-1, (10.1109/TPWRD.2020.3031277)

[26] A. Rafinia, J. Moshtagh, "A new approach to fault location in three-phase underground distribution system using combination of wavelet analysis with ANN and FLS", IJEPES, 55, 261-274, 2014

[27] Z. Tong, L. Xianhong, Y. Haibin, L. Jianchang, Z. Peng, S. Lanxiang, "A fault location method for active distribution network with renewable sources based on BP neural network", 7th International conference on Intelligent human-machine systems and cybernetics, Hangzhou, China 2015

[28] Y. Li, Y. Zhang, W. Liu, Z. Chen. Y Li, J. Yang, "A fault pattern and convolutional neural network based on single-phase earth fault identification method for distribution network", IEEE Innovative Smart Grid Technologies - Asia (ISGT Asia), Chengdu, China, 2019

[29] CIGRE Technical Brochure 773, "Fault location on land and submarine links (AC & DC) ", WG B1.52, September 2019

[30] M. Shafiq, G. A. Hussain, L. Kutt, N. I. Elkalashy, "Partial discharge diagnostic system for smart distribution networks using directionally calibrated induction sensors", EPSR 119 (2015) 447-461

[31] M. Benitez, J. Xavier, K. Smith, D. Minshall, "Directional element design for protecting circuits with capacitive fault and load currents", 71st Annual Conference for Protective Relay Engineers (CPRE), College Station, TX, USA. 2018

[32] T. Kelemen, "Ferroresonance In Networks With Isolated Neutral", 4th HK CIGRÉ, Group 12 – Transformers, 17.-21.10.1999., Cavtat, Croatia

[33] Technical Data, SIPROTEC 5, Overcurrent Protetion 7SJ82/7SJ85, Manual c53000-G5040-C017-8, Edition 11.2017SIEMENS

[34] IEC 61869-2 :2012, Instrument transformers - Part 2: Additional requirements for current transformers

[35] Vigilohm datasheet, "Mobile fault locating kit." [Online]. Available: http://www.naewoielec.co.kr/pdf/XRMXGR01.pdf. [Accessed: 27-Aug-2020]